Tuning the Magnetic Interactions in Dy(III)4 Single-Molecule Magnets

Kun Zhang, Vincent Montigaud, Olivier Cador, Gao-Peng Li, Boris Le Guennic, Jin-Kui Tang, Yao-Yu Wang

Tuning the Magnetic Interactions in $Dy(III)_4$ Single-Molecule Magnets

Kun Zhang,[a,b] *Vincent Montigaud,*[d] *Olivier Cador,*[d] *Gao-Peng Li,*[b] *Boris Le Guennic,**[,d] *Jinkui Tang**[,c] *and Yao-Yu Wang**[,b]

[a] School of Textile Science and Engineering, Xi'an Polytechnic University, Xi'an 710048, P. R. China.

[b] Key Laboratory of Synthetic and Natural Functional Molecule Chemistry of the Ministry of Education, Shaanxi Key Laboratory of Physico-Inorganic Chemistry, College of Chemistry & Materials Science, Northwest University, Xi'an, 710127, P. R. China.

[c] State Key Laboratory of Rare Earth Resource Utilization, Changchun Institute of Applied Chemistry, Chinese Academy of Sciences, Changchun 130022, P. R. China.

[d] Univ Rennes, CNRS, ISCR (Institut des Sciences Chimiques de Rennes) - UMR 6226, F-35000 Rennes, France.

ABSTRACT:

The study of mononuclear lanthanide-based systems, where the observed Single Molecule Magnets (SMMs) properties originate from the local description of the magnetic properties of the lanthanide ion, has been widely investigated through the literature. The case of polynuclear SMMs becomes more challenging both experimentally and theoretically due to the complexity of such architectures involving interactions between the magnetic centers. Many efforts have been focused on the understanding of the nature of these interactions and their effects on the SMM properties. In this work, a series of three structurally related tetranuclear dysprosium(III) SMMs, namely $[Dy_4(L)_4(OH)_2(DMF)_4(NO_3)_2]\bullet 2(DMF)\bullet(H_2O)$ (**1**), $[Dy_4(L)_4(OH)_2(DMF)_2(tfaa)_2]\bullet 2(CH_3CN)$ (**2**) and $[Dy_4(L)_4(OH)_2(DMF)_2(acac)_2]\bullet 2(DMF)$ (**3**) (H_2L = 2-(2-hydroxy-3-methoxybenzylideneamino)phenol, Htfaa = trifluoroacetylactone, Hacac = acetylacetonate), has been synthesized and investigated. By a fine-tuning of the ligands on the changeable coordination sites in these $Dy(III)_4$ SMMs, the intramolecular magnetic interactions can be modified, switching from antiferromagnetic (for **1** and **2**) to ferromagnetic (for **3**). *Ab initio* calculations support these statements. In addition, the formation of **1** has been analyzed by ESI-MS analysis of the reaction mixture, indicating rather quick and high-yield formation of the $[Dy_4]$ framework in solution. The combination of experimental work and *ab initio* calculations offers further insight into the relationship between structures and magnetic properties and sheds light on how to tune magnetic interactions in future polynuclear dysprosium complexes.

1. INTRODUCTION

Dysprosium(III) ion, benefiting from its significant magnetic anisotropy and Kramers doublet ground state, has shown to be an appealing candidate for building polynuclear single-molecule magnets (SMMs) that can be potentially applied in ultrahigh-density information storage, quantum computing and molecular spintronics.[1-5] The recent advance made by Goodwin, Mills and co-workers in mononuclear dysprosium (III) SMMs, whereby the magnetic hysteresis and effective energy barrier reach up to 60 K and 1760 K respectively, have showed the great potential of dysprosium (III) SMMs in the application of molecule-based magnetic storage materials.[6-7] Therefore, interest towards obtaining high-performance dysprosium (III) SMMs has been continuously growing. In this regard, efforts are increasingly devoted to exploring the magneto-structural correlations of dysprosium (III) SMMs, which have been proposed as the basis of directing the structural optimization of magnetic properties.[8-11] The effective strategies in this respect are toward modifying the geometry and charge distribution on metal site combined with theoretical calculations to illustrate the structural effect on the magnetic properties, and this was well demonstrated in mononuclear dysprosium (III) SMMs.[12-20] However, due to the presence of magnetic interactions between metal centers, the case becomes more complicated for systems encapsulating two or more dysprosium (III) ions,[21-26] for which magnetic phenomena become hardly predictable. Even so, understanding the relationship between the magnetic interactions and molecular structures becomes more important when such interactions have been shown to improve the magnetic relaxation properties in few dysprosium (III) complexes.[27-29] Although difficult, it has been showed that the magnetic interactions are extremely sensitive to the subtle variations of the local coordination sphere and the ligand field around the dysprosium (III) ion.[30-31] A current challenge, therefore, is to assemble targeted polynuclear dysprosium (III)

SMMs, thereby providing a means of tuning the magnetic interactions through the influence of different coordination environments around the metal site.

In this contribution, we demonstrate how the magnetic interactions in polynuclear dysprosium(III) SMMs can be modified by structural changes. Specifically, three structural related tetranuclear dysprosium(III) SMMs, namely $[Dy_4(L)_4(OH)_2(DMF)_4(NO_3)_2]\bullet 2(DMF)\bullet(H_2O)$ (**1**), $[Dy_4(L)_4(OH)_2(DMF)_2(tfaa)_2]\bullet 2(CH_3CN)$ (**2**) and $[Dy_4(L)_4(OH)_2(DMF)_2(acac)_2]\bullet 2(DMF)$ (**3**) (H_2L = 2-(2-hydroxy-3-methoxybenzylideneamino)phenol, Htfaa = trifluoroacetylactone, Hacac = acetylacetonate), are synthesized and investigated for structure-dependent magnetic properties. The key feature of these complexes is that four Dy(III) ions are nearly coplanar in a regular parallelogram, forming a distorted defective dicubane $\{Dy_4O_8\}$ core with two crystallographically independent Dy(III) ions (Dy1/Dy1a and Dy2/Dy2a). By tuning the geometry (from nine-coordinated to eight-coordinated) and charge distribution (from $tfaa^-$ to $acac^-$) of the ligand on the changeable coordination site Dy1/Dy1a, the magnetic properties showed a modification of the intramolecular magnetic interactions, switching from antiferromagnetic to ferromagnetic. As elucidated by *ab initio* calculations, the coordination environment surrounding the changeable metal site plays a key role in the magnetic interactions. In addition, the formation of **1** was analyzed by ESI-MS indicating rather quick and high-yield formation of the $[Dy_4]$ framework in solution and provided information about changeable coordination sites.

2. RESULTS AND DISCUSSION

2.1 Syntheses and Characterizations.

2-(2-hydroxy-3-methoxybenzylideneamino)phenol (H_2L) is a multidentate Schiff base ligand in which the coordinating atoms are located on the same side of the molecule, which favors bridging two or more ions to form polynuclear complexes (Figure 1 inset).[32-34] In this study, structurally related **1**-**3** were isolated using the stepwise synthetic approach. First, $[Dy_4(L)_4(OH)_2(DMF)_4(NO_3)_2]$•2(DMF)•($H_2O$) (**1**) was prepared from $Dy(NO_3)_3$•$6H_2O$, H_2L and trimethylamine (NEt_3) following a solvent evaporation procedure reported in previous work.[35-38] Then, the synthesis of **1** is repeated and a replacing ligand, trifluoroacetylactone (Htfaa), is added to the reaction solution resulting in the formation of $[Dy_4(L)_4(OH)_2(DMF)_2(tfaa)_2]$•2($CH_3CN$) (**2**, Figure 1). Finally, complex $[Dy_4(L)_4(OH)_2(DMF)_2(acac)_2]$•2(DMF) (**3**) (Figure 1), was synthesized in the same way as for complex **2** with acetylacetonate (Hacac) as modified axial ligand (instead of Htfaa for **2**). Powder X-ray diffraction (PXRD) patterns match well with those calculated using the single-crystal X-ray data, which confirms the formulations and phase purity of the bulk product (Figure S1 in the Supporting Information).

2.2 Crystallography Structures.

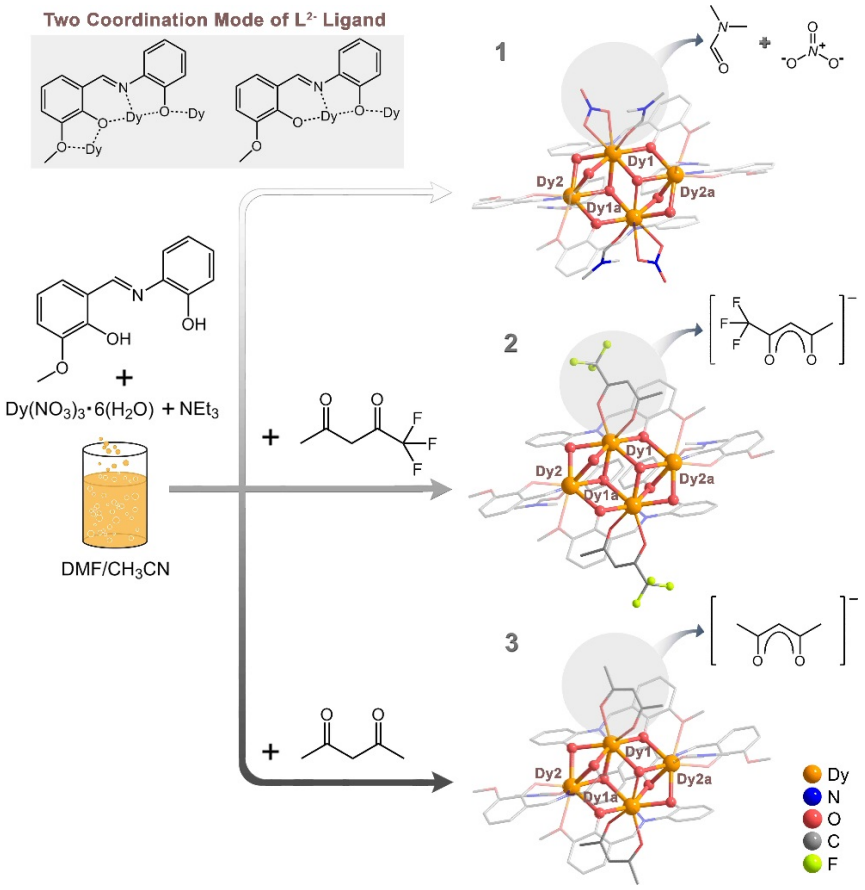

Figure 1. The genealogy of the complexes **1**-**3** follows the solvent evaporation route. The $\{Dy_4O_8\}$ core and the modification of ligands on the Dy1 and Dy1a sites were highlighted. Hydrogen atoms and solvent molecules have been omitted for clarity. Inset: The two coordination mode of L^{2-} Ligand

Following a solvent evaporation procedure at ambient condition, a tetranuclear complex $[Dy_4(L)_4(OH)_2(DMF)_4(NO_3)_2]$•2(DMF)•($H_2O$) (**1**) was obtained. It is crystallographically centrosymmetric and crystallizes in the monoclinic space group $P2_1/n$ (Figure 1). The key feature of this complex is that four Dy(III) ions are nearly coplanar in a regular parallelogram, forming a distorted defective dicubane $\{Dy_4O_8\}$ core (Figure 1). In each of the two symmetry-related $Dy_2(L)_2$ moieties, two Dy(III) ions (Dy1 and Dy2 or Dy1a and Dy2a) are linked by two μ_2-

phenoxo oxygen atoms from two symmetry equivalent L^{2-} ligands, and the moieties are further linked by two μ_3-hydroxide ligands with the Dy1···Dy2 distances of 3.4935(8) Å (Table S2). The Dy1 atom is nine-coordinated and bounded by the $\{NO_8\}$ environment made of one N atom and three phenoxo O atoms from L^{2-} ligands and two μ_3-hydroxide O, two nitrate O and one DMF O, adopting a distorted tricapped trigonal prism geometry (Table S3). The Dy2 atom has a distorted square-antiprism eight-coordinated $\{NO_7\}$ environment which is completed by one N atom and four phenoxo O atoms from L^{2-} ligands and one μ_3-hydroxide O, one methoxide O and one DMF O. The complexes are surrounded by solvent water and DMF molecules that prevent any inter-complex π–π stacking and the intermolecular Dy···Dy distances are over 10 Å. It is worth noticing that in the other $[Dy_4]$ parallelogram cases, the majority metal sites display eight-coordinated environment only,[32-33, 39-42] while in some unusual cases, two metal sites are seven-coordinated with two being eight-coordinated,[43] two eight with two nine,[44-45] and two nine with two ten.[46] Thus the present complex adds another example into this unusual catalog.

The structure of **2** could be seen as a derivative of **1** by replacing the axial DMF and NO_3^- with the trifluoroacetylactone ($tfaa^-$) ligand on changeable coordination Dy1/Dy1a sites. In this new configuration, the previous nine-coordinated Dy1 and Dy1a ions became eight-coordinated, which are surrounded by the $\{NO_7\}$ environment build with one N atom and three phenoxo O atoms from L^{2-} ligands and two μ_3- hydroxide O, two nitrate O, adopting a distorted biaugmented trigonal prism geometry (Table S3). While the coordination sphere of the Dy2/Dy2a ions maintained the same coordination number and surrounded by the same coordination atoms.

To modify the coordination environments of the sites thus tuning the magnetic properties, complex **3** $[Dy_4(L)_4(OH)_2(DMF)_2(acac)_2]\bullet 2(DMF)$ (Figure 1), was synthesized with acetylacetonate (Hacac) as modified axial ligand (instead of Htfaa for **2**). The $acac^-$ ligands (in **3**)

replaced tfaa$^-$ ligands (in **2**) to complete the eight-coordinated sphere of Dy1/Dy1a while retaining the same kind of coordination atoms, which exhibits a distorted biaugmented trigonal prism geometry C_{2v}. The coordination sphere of the Dy2/Dy2a ions maintained the same coordination number and surrounded by the same coordination atoms. The continuous shape measures to a biaugmented trigonal prism C_{2v} of Dy2 determined by SHAPE software[47] reveal very similar coordination spheres of the Dy2 ion in **2** and **3** (Table S3). Besides, only small structural variations for the $\{Dy_4O_8\}$ core were found in complex **3** when compared to **2** (Table S2). It should be noted that the key difference in these two structures is the modification of the charge distribution on the caping ligands, the variation from tfaa$^-$ to acac$^-$ on the axial positions of the Dy1/Dy1a ions increases the negative average charge (Figure 1). Such structural variations are most likely responsible for the transition of magnetic interactions (*vide infra*). Additionally, the structures of **1**-**3** are also similar to the reported structure of $[Dy_4(L)_4(OH)_2(DMF)_2(NO_3)_2]$, in which the DMF on the Dy1/Dy1a in **1** removed, tfaa$^-$ and acac$^-$ in **2** and **3** replaced by NO_3^- ligand.[33]

2.3 ESI-MS Analysis of the Formation of 1.

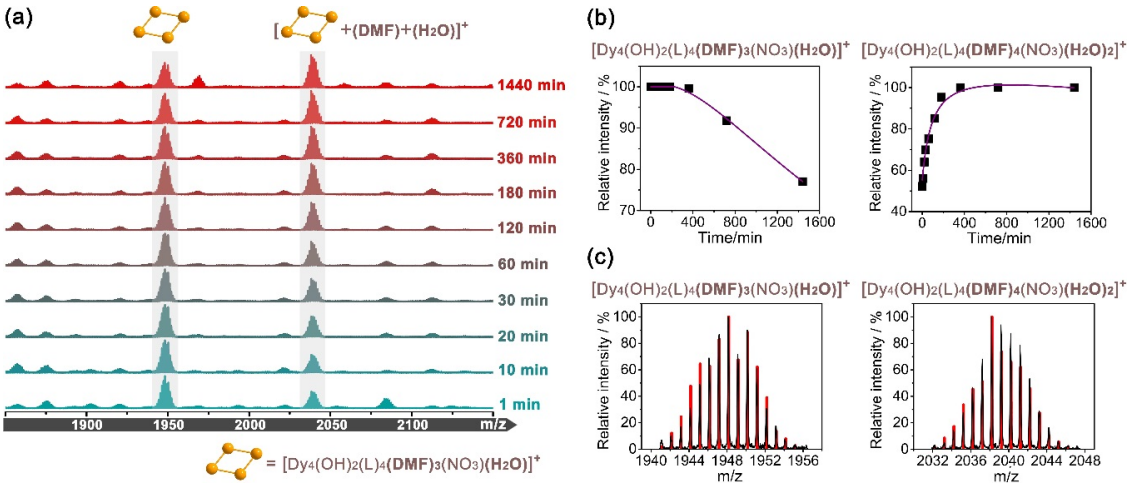

Figure 2. (a) Time-resolved ESI-MS spectra with two reactant-related and product-related $[Dy_4]^+$ species. (b) The general trends of normalized peak intensity of the representative species over time. Purple color lines of best fit are shown as a guide for the eye only. (c) Red bars represent the simulated spectra and black lines represent the experimental spectra choose from 1440 min (Figure S3).

To give more insight into the formation of complex **1**, a ESI-MS study of the different species present in solution depending on the reaction time was performed (Figure 2). Analysis of the first ESI-MS spectrum showed that the very strong $[Dy_4]^+$ species appeared within the reaction time of 1 min, which indicated the formation of the $[Dy_4]$ framework quickly and highly-yield (Figure 2a). The most dominated peak in spectrum can be assigned to $[Dy_4(OH)_2(L)_4(DMF)_3(NO_3)\ (H_2O)]^+$ (denoted as $[Dy_4(DMF)_3]$) by well matching experimental spectra with simulated one (Figure S2), corresponding to the intact molecular species of **1** losing one coordinated NO_3^- ligand (to yield the necessary positive m/z during the ESI-MS process), one coordinated DMF (replaced by H_2O), as well as all solvent molecules. Interestingly, compared to crystallographic structure of **1**, the nearby relative lower intensity envelopes of $[Dy_4(OH)_2(L)_4(DMF)_4(NO_3)(H_2O)_2]^+$ (denoted as $[Dy_4(DMF)_4]$) founded within the same time window could be seen as the product-related species in solution, which may suggest that the coordination sphere of Dy(III) were further completed by adding DMF molecule to the intermediate $[Dy_4(DMF)_3]$ species.

Further information about the formation of **1** taking place in solution, from the intermediate $[Dy_4(DMF)_3]$ species to the product-related $[Dy_4(DMF)_4]$, can be reliably extracted from the ESI-MS data by monitoring the reaction process as a function of time.[48-49] To this end, the evolution of the relative intensity of the peaks corresponding to these two species over time is presented in

Figure 2b. The relative intensity of the intermediate [$Dy_4(DMF)_3$] species gradually decreased (from 1 min to 20 h), whilst the intensity of the product-related [$Dy_4(DMF)_4$] species significantly increased within initial 3h reaction time and remained unchanged till the end of the reaction (after 24h, crystals of **1** have already started to form at the bottom of reaction flask). The study of the solution dynamics through the ESI-MS technique coupled with the solid-state structure analysis allowed a better understanding of the self-assembly process of **1** in solution. The coordination of the ligands L^{2-} to the Dy(III) ions results in the formation of a relatively stable [$Dy_4(DMF)_3$] species owning changeable coordination sites Dy(III) sites for which the coordination environment could be further modified by adding coordinated DMF molecule resulting in the [$Dy_4(DMF)_4$] species in solution and eventually leading to the crystallization of solid **1**.

2.4 Magnetic Properties.

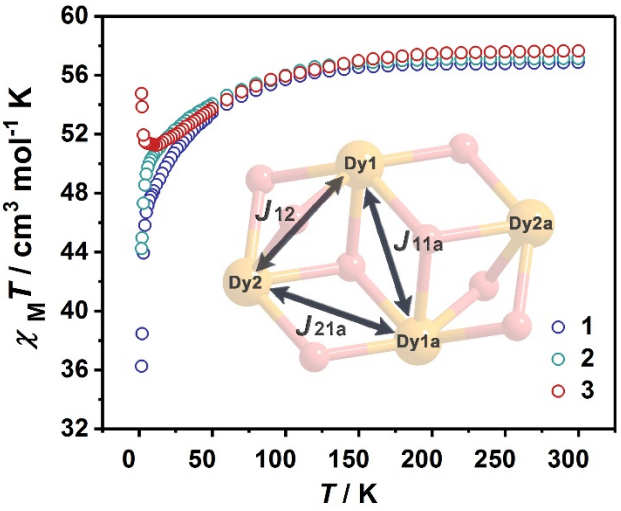

Figure 3. Curves of the $\chi_M T$ versus temperature for complexes **1**-**3** under an applied dc field of 500 Oe. Inset: Schematic representation of the contributions of exchange interactions considered in the calculations.

The direct current (dc) magnetic susceptibilities for complexes **1-3** are measured under an applied dc field of 500 Oe from 300 K to 1.8 K (Figure 3). The microcrystalline of **1-3** was fixed into eicosane, which are placed inside a polycarbonate capsule. Both the contributions of the eicosane and the capsule were subtracted. At 300 K, the $\chi_M T$ values of complexes **1-3** are 56.86, 57.13 and 57.64 cm^3 K mol^{-1}, respectively, which are close to the expected value (56.68 cm^3 K mol^{-1}) for four non-interacting Dy(III) ions.[50] With temperature cooling, the $\chi_M T$ values of **1** and **2** undergo a gradual reduction from 300 K to 50 K, followed by a sudden decrease to a minimum value of 36.26 and 44.23 cm^3 K mol^{-1} at 1.8 K, respectively. The decrease of $\chi_M T$ upon the temperature cooling can be attributed to the thermal depopulation of the m_J levels of the ground state of the Dy(III) ions and/or the possible antiferromagnetic interactions between the metal centers, which is in agreement with reported similar Dy(III) complexes.[51-52] For **3**, the $\chi_M T$ curve gradual decrease to 51.26 cm^3 K mol^{-1} at 12 K, then increased rapidly to a maximum of 54.75 cm^3 K mol^{-1} at 1.8 K. The increase of $\chi_M T$ at low temperature suggests the presence of ferromagnetic interactions between the Dy(III) ions.

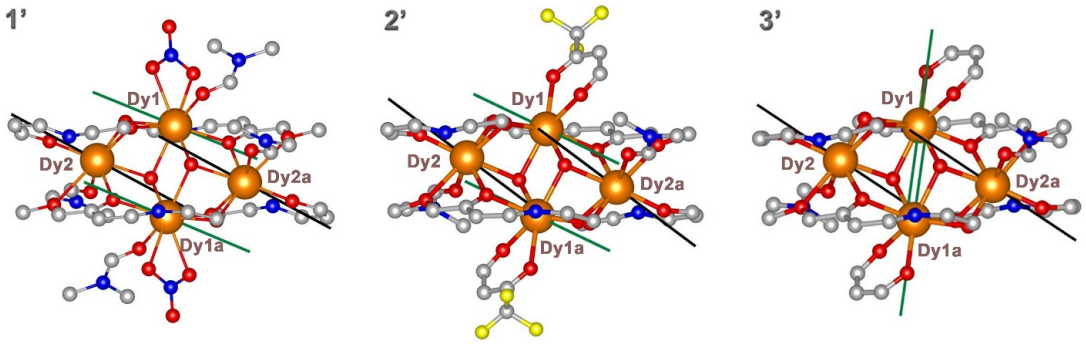

Figure 4. Schematic representation of the highest g tensor component of each Dy center, green line for Dy1 and Dy1a and black line for Dy2 and Dy2a, for the model complexes **1'-3'**. Dy, O, N, F and C atoms are in orange, red, blue, yellow and grey, respectively. H atoms are omitted for clarity.

To rationalize the direct current magnetic measurements for the two complexes, *ab-initio* SA-CASSCF/SI-SO calculations were performed on models **1'** - **3'** using the Molcas 8.0 program package (Figure 4 and computational details in Supporting Information).[53] $\chi_M T$ in the temperature range of 2-300K are presented in Figure S4 – S6 for **1** - **3**, respectively. A first set of calculations was performed without considering the exchange interactions (J_{ex}) between the Dy(III) centers, *i.e*. only considering dipolar couplings (J_{dip}). The calculated values of $\chi_M T$ reproduced the decrease upon cooling observed for complexes **1** and **2** before reaching a minimum value of 52.07 cm^3 K mol^{-1} at 18 K and 49.93 cm^3 K mol^{-1} at 12 K for **1'** and **2'** respectively (model complexes, Figure 4). The $\chi_M T$ values then increase upon further cooling to reach a value of 73.61 cm^3 K mol^{-1} at 2 K for **1'** and 53.63 cm^3 K mol^{-1} at 2 K for **2'**. The strong increase of the $\chi_M T$ values observed at low temperature can be attributed to ferromagnetic interactions between the Dy(III) centers. In the opposite, for **3'**, a decrease from room temperature to low temperature is observed, reaching the value of 35.7 cm^3 K mol^{-1} at 2K (Figure S6). This different behavior can be attributed to antiferromagnetic dipolar interactions between the magnetic centers. Clearly, contrary to experimental results, the theoretical description of the low temperature behavior of all three complexes misses some important components at this stage that may be ascribed to exchange interactions. These exchange interactions are considered in subsequent calculations ($J_{dip} + J_{ex}$) in order to balance the dipolar coupling contributions (Jdip). These exchange parameters are fitted to obtain the best

agreement with the experimental dc magnetic data (Figures S4-S6). The different components of the exchange interaction contributions that are considered are shown in Figure 3 inset. The exchange interaction between the Dy2 and Dy2a centers (J_{22a}) is not considered in the calculations due to the large Dy···Dy distance and the lack of bridging ligands. The best fitted exchange values are reported in Table 1.

In all complexes, the magnetic exchange contributions between the two nonequivalent Dy(III) centers (Dy1 and Dy2) are antiferromagnetic ($J_{12} < 0$) while J_{11a} is ferromagnetic (Figure 3 inset). The change of the coordination sphere around Dy1/1a, from nine-coordinated in complex **1** to eight-coordinated in **2**, leads to a strong decrease of J_{21a} (Table 1). The low temperature $\chi_M T$ behavior observed for **1** and **2** is explained by the major antiferromagnetic exchange contribution to the overall intramolecular Dy···Dy interactions that dominates the ferromagnetic contributions coming from both the dipolar coupling and the J_{11a} exchange contribution. Then, efforts have been focused on the fine tuning of the axial ligand, located on the Dy1/1a center, in order to influence the intramolecular magnetic interactions, leading to complex **3**. The results show that the increase of the negative charge on the axial ligand observed for **3** strengthens the exchange interactions between the Dy centers. Contrary to complexes **1** and **2**, complex **3** exhibits antiferromagnetic dipolar interactions (Figure S6). The opposite contributions of both the dipolar coupling and the J_{12} exchange contribution are balanced by the increased ferromagnetic contributions from the J_{21a} and J_{11a} exchange components resulting in the increase of the $\chi_M T$ observed at low-temperature for complex **3**.

Table 1. Best fitted exchange values (cm^{-1}, in the Ising model) for model complexes **1'**, **2'** and **3'** within the scan range -2.5 – +2.5 cm^{-1}.

Complex	J_{12} (cm^{-1})	J_{21a}(cm^{-1})	J_{11a} (cm^{-1})
1'	-1.75	-2.5	1
2'	-1.75	0.25	0.75
3'	-2.5	2.5	2.5

The field (*H*) dependence of the magnetization (*M*) of complexes **1** - **3** at 2 K, 3 K and 5 K shows a rapid increase of the magnetization at low fields followed by a linear gradual increase at high fields without reaching the saturation of 40 Nβ (Figure S7). The high field non-saturation combined with the non-superposition of the *M* vs HT^{-1} curves on a single master-curve (Figure S8) suggests the presence of significant magnetic anisotropy and/or low lying excited states as expected for Dy(III) ions.[54] There are no hysteresis detected for **1** - **3** at 1.8 K (Figure S9).

In order to investigate the dynamic properties of the magnetization, ac susceptibility measurements for complexes **1** - **3** under zero dc field were performed. Ac magnetic susceptibility studies show an obvious frequency dependence of out-of-phase (χ_M''), indicating slow relaxation of the magnetization and the SMM behaviors for complexes **1** - **3** (Figures S10-S11).[55] However, for complex **1**, as the temperature decreases to 2 K, no maximum was observed for the χ_M'' values, which indicates that the blocking temperature of the spin reversal should below 2 K. As shown in Figure S10 and S11, two regimes of relaxation are observed for **2** and **3**, which may be attributed to the presence of two individual Dy centers with different intrinsic magnetic anisotropies (Dy1 and Dy2).[56] To further understand the connection of the relaxation process and corresponding Dy(III) ions for **2** and **3**, it is necessary to provide a closer comparison between the χ_M'' curves of the two complexes(Figure 5). Obviously, the significant difference is shown in the high-temperature relaxation processes, while the similar in low-

temperature relaxation processes. Take the curves of 299 and 997 Hz as examples, complexes **2** and **3** exhibit a very similar relaxation processes in the low-temperature, whereas the maximum value of χ_M'' for the high-temperature relaxation move to higher temperatures from **2** and **3** (Figure 5). Therefore, the low-temperature relaxation process could be connected to the Dy2 center due to their almost identical coordination sphere in the two complexes, and the move in the high-temperature relaxation process could be considered as the result of the local modification of coordination environment on the Dy1 site. These assignments are further confirmed by *ab-initio* calculations on model complexes **1'-3'** (*vide infra*). From table S10-S17, the energy difference between the ground and the first excited state and the anisotropic features of the Dy2 ions were found almost identical for **2'** and **3'**, which indeed support the very similar low-temperature relaxation processes. The sharp increase of energy splitting at the Dy1 site from **2'** to **3'** lead to the obvious move of the χ_M'' signals in the high-temperature relaxation process.

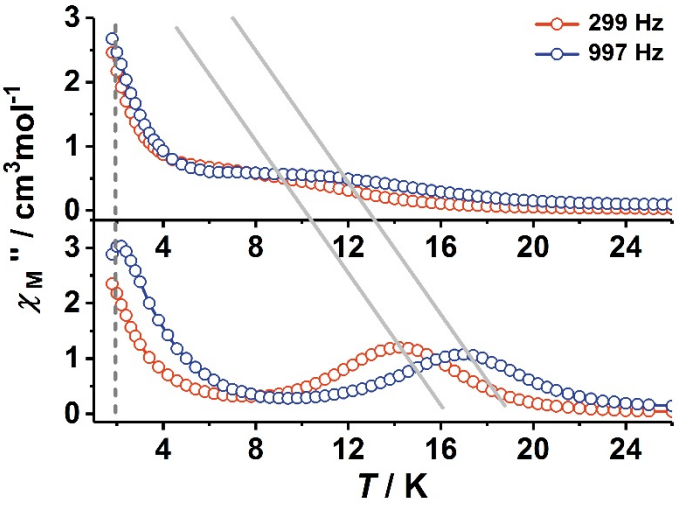

Figure 5. The temperature dependent ac susceptibility of χ_M'' for complexes **2** (top) and **3** (bottom). The dashed-line indicates the very similar low-temperature relaxation process for the two complexes. The solid lines indicate the move in the high-temperature relaxation process.

Also, well-separated two-step relaxation processes are observed in the frequency-dependent out-of-phase χ_M'' measurements, which correspond to the fast relaxation process (FR) and slow relaxation process (SR), respectively(Figures S12 and S14). The relaxation times for FR (τ_1) and SR(τ_2) can be determined by fitting the frequency-dependent χ_M'' curves to two relaxation processes by employing the Debye functions (Figures S13 and S15, Tables S4 and S5). The plot of $\ln\tau_2$ *versus* T^{-1} was obtained to get deeper understanding about the slow relaxation processes of **2** and **3**. As seen in Figure 6, an obvious curvature showed in the plot, indicating that other relaxation pathways occurred. It is worth noting that other relaxation processes, such as Raman process, can coexist with Orbach relaxation. Therefore, the data over the entire temperature range were analyzed by the following equation (1):

$$\ln\tau = -\ln[CT^n + \tau_0^{-1}\exp(-U_{eff}/k_BT)] \quad (1)$$

where the two terms represent the Raman and Orbach processes, respectively (C is the coefficient of Raman process, U_{eff} is the energy barrier to magnetization reversal, and k_B is the Boltzmann constant). Figure 6 shown the best fittings, giving C = 15.1 s^{-1} $K^{-1.7}$, n = 1.7, $\tau_0 = 2.09 \times 10^{-5}$ s, U_{eff}/k_B = 39 K for **2** and C = 0.35 s^{-1} $K^{-2.4}$, n = 2.4, $\tau_0 = 9.62 \times 10^{-7}$ s, U_{eff}/k_B = 94 K for **3**. The obtained τ_0 values within the range between 10^{-5} and 10^{-12} s are expected for the polynuclear dysprosium SMMs.[57] In addition, the effective barrier of **3** is much higher than that of complex **2**, in good agreement with the increase of energy splitting between the ground and the first excited state resulting from the local modifications of the coordination environment at the Dy1 site from **2** to **3** (Tables S10-S17).

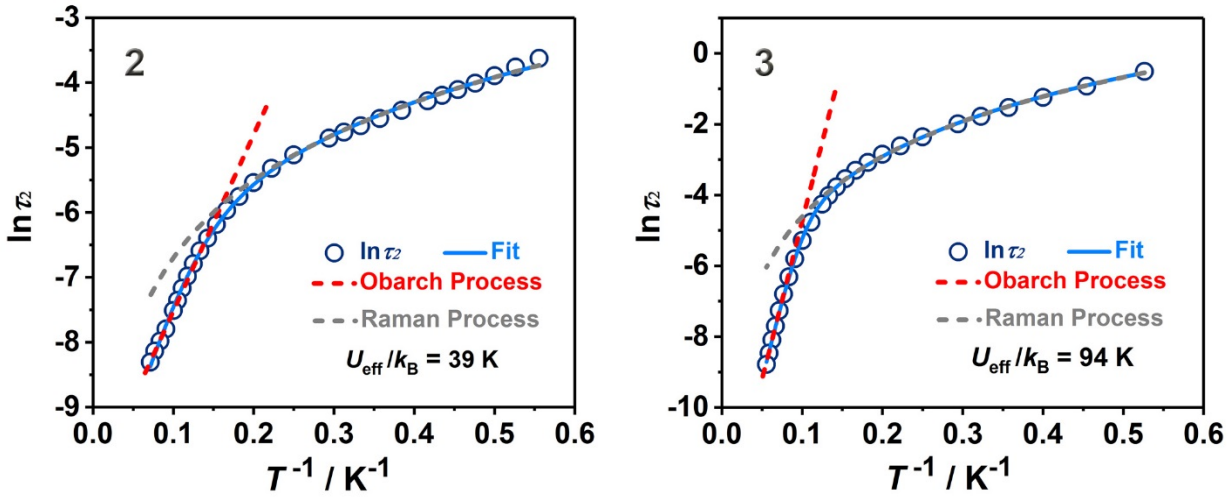

Figure 6. Plots of ln(τ_2) versus T^{-1} for **2** and **3**, where τ_2 is the relaxation time, T refers to the temperature (K). The blue line represents the fit to multiple relaxation processes using the eqn (1).

To rationalize the differences observed in the relaxation dynamics of complexes **1**, **2** and **3**, further SA-CASSCF/SI-SO calculations were performed on models **1'** – **3'** (Figure 4). In the effective spin ½ approximation, the principal components of the g tensor and the wavefunction composition of the ground state multiplet are calculated for each Dy centers of each model complexes **1' – 3'** (Tables S6-S17). In all model complexes, the Dy2 and Dy2a centers exhibited an almost pure (96%) |±15/2⟩ ground state with an Ising type, strongly axial anisotropy ($g_X = g_Y$ = 0.01 and g_Z around 19.7). For Dy1 and Dy1a (the metal centers with varying coordination numbers) a similar behavior was found in model complexes **1'** and **3'**. Indeed, a mixed ground state with a major contribution of the |±15/2⟩ spin states (0.77 |±15/2> + 0.15 |±11/2> for Dy1 of **1'** and 0.86 |±15/2> + 0.11 |±11/2> for **3'**). The calculated ground state g tensor (g_X = 0.49, g_Y = 1.22, g_Z = 18.06 for **1'** and g_X = 0.22, g_Y = 0.73, g_Z = 18.82 for **3'**) was found to be axial but lacks pure Ising nature. A quite different behavior was observed for the Dy1 and Dy1a centers of **2'** with a mixed ground state (0.57 |±15/2> + 0.14 |±11/2> + 0.07 |±9/2>) giving rise to ground state

g-values of g_X = 1.41, g_Y = 4.54 and g_Z = 14.01 characterizing a low magnetic anisotropy on the Dy1 center. The orientation of the main g-values (g_Z components) of each Dy center are represented in Figure 4. As expected, due to the small variations of the Dy2/2a coordination spheres, very small deviations of the magnetic anisotropy axis are observed between the three complexes. To the contrary, the non-negligible variation of the coordination sphere around the Dy1/1a centers led to remarkable deviation of the magnetic anisotropy axis orientation between **1'** and **3'**. In order to give further insights into the magnetic anisotropy axis orientation, a home-made program (CAMMEL, see Supporting Information) allowing to map the electrostatic potential around the chosen Dy center has been used on model complexes **1'** and **3'** (Figure S16-18). The representation of each component of the total potential (charge, dipole and quadrupole) revealed the major contribution of the quadrupole component to the total potential. In **1'**, the magnetic axis is oriented in a minimum of potential generated by an O atom of a ligand L forming the $\{Dy_4O_8\}$ core. The increase of the negative charge on the O atoms of the axial ligand (acac) in **3'**, lowered the potential generated by these O atoms allowing a switch of the magnetic axis from an O atom of the $\{Dy_4O_8\}$ core to an O from the axial ligand (Figure 4).

3. CONCLUSION

In summary, structural variations within three tetranuclear Dy(III) SMMs have been showed to be an important factor in tuning the magnetic interactions. *Ab initio* calculations revealed the magnetostructural relationship in such complexes. That is, the modification of coordination sphere (from nine-coordinated in **1** to eight-coordinated in **2**) and the charge distribution of the axial ligand (from $tfaa^-$ in **2** to $acac^-$ in **3**) on the changeable coordination Dy1/Dy1a sites can significantly affect the exchange interactions between the Dy(III) centers, and thus causing a

transition of magnetic interactions from antiferromagnetic to ferromagnetic. This offers new strategies for tuning magnetic interactions in future lanthanide complexes.

ASSOCIATED CONTENT

Supporting Information. Experimental details, elemental analyses, IR, PXRD, X-ray Crystallography information, ESI-MS, magnetic data, computational details. "This material is available free of charge via the Internet at http://pubs.acs.org.". CCDC 1830054 for complex **1**, 1830055 for **2** and 1830056 for **3** contain the supplementary crystallographic data for this paper. CIF files can be obtained free of charge from the Cambridge Crystallographic Data Centre via www.ccdc.cam.ac.uk/data_request/cif.

AUTHOR INFORMATION

Corresponding Author

*wyaoyu@nwu.edu.cn

*tang@ciac.ac.cn.

*boris.leguennic@univ-rennes1.fr

Notes

The authors declare that they have no competing financial interests.

ACKNOWLEDGMENT

This work was supported by the NSFC (Grants 21371142, 21531007, 21525103 and 21521092), the NSF of Shaanxi Province. B.L.G. thanks the French GENCI/IDRIS-CINES center for high-performance computing resources.

REFERENCES

(1) Gatteschi, D. Anisotropic Dysprosium. *Nat. Chem.* **2011**, *3*, 830.

(2) Sorace, L.; Benelli, C.; Gatteschi, D. Lanthanides in Molecular Magnetism: Old Tools in a New Field. *Chem. Soc. Rev.* **2011**, *40*, 3092–3104.

(3) Woodruff, D. N.; Winpenny, R. E. P.; Layfield, R. A. Lanthanide Single-Molecule Magnets. *Chem. Rev.* **2013**, *113*, 5110–5148.

(4) Tang, J. K.; Zhang, P. *Lanthanide Single Molecule Magnets*, Springer, Berlin, Heidelberg, **2015**.

(5) Kiefl, E.; Mannini, M.; Bernot, K.; Yi, X.; Amato, A.; Leviant, T.; Magnani, A.; Prokscha, T.; Suter, A.; Sessoli, R.; Salman, Z.; Robust Magnetic Properties of a Sublimable Single-Molecule Magnet. *ACS Nano*, **2016**, *10*, 5663–5669.

(6) Goodwin, C. A. P.; Ortu, F.; Reta, D.; Chilton, N. F.; Mills, D. P. Molecular Magnetic Hysteresis at 60 K in Dysprosocenium. *Nature* **2017**, *548*, 439–442.

(7) Guo, F. S.; Day, B. M.; Chen, Y. C.; Tong, M. L.; Mansikkamaki, A.; Layfield, R. A. A Dysprosium Metallocene Single-Molecule Magnet Functioning at the Axial Limit. *Angew. Chem. Int. Ed.* **2017**, *56*, 11445–11449.

(8) Rinehart, J. D.; Long J. R. Exploiting Single-Ion Anisotropy in the Design of F-Element Single-Molecule Magnets. *Chem. Sci.* **2011**, *2*, 2078–2085.

(9) Chilton, N. F.; Collison, D.; McInnes, E. J. L.; Winpenny, R. E. P.; Soncini, A. An Electrostatic Model for the Determination of Magnetic Anisotropy in Dysprosium Complexes. *Nat. Commun.* **2013**, *4*, 2551.

(10) Zhang, P.; Guo, Y. N.; Tang, J. K. Recent Advances in Dysprosium-Based Single Molecule Magnets: Structural Overview and Synthetic Strategies. *Coord. Chem. Rev.* 2013, **257**,

1728–1763.

(11) Liu, J. L.; Chen, Y. C.; Tong, M. L. Symmetry Strategies for High Performance Lanthanide-Based Single-Molecule Magnets. *Chem. Soc. Rev.* **2018**, *47*, 2431–2453.

(12) Jiang, S. D.; Wang, B. W.; Su, G.; Wang, Z. M.; Gao, S. A Mononuclear Dysprosium Complex Featuring Single-Molecule Magnet Behavior. *Angew. Chem. Int. Ed.* **2010**, *49*, 7448–7451.

(13) Chen, G. J.; Guo, Y. N.; Tian, J. L.; Tang, J.; Gu, W.; Liu, X.; Yan, S. P.; Cheng, P.; Liao, D. Z. Enhancing Anisotropy Barriers of Dysprosium(III) Single-Ion Magnets. *Chem.-Eur. J.* **2012**, *18*, 2484–2487.

(14) Cucinotta, G.; Perfetti, M.; Luzon, J.; Etienne, M.; Car, P.-E.; Caneschi, A.; Calvez, G.; Bernot, K.; Sessoli, R. Magnetic Anisotropy in a Dysprosium/DOTA Single-Molecule Magnet: Beyond Simple Magneto-Structural Correlations. *Angew. Chem., Int. Ed.* **2012**, 51, 1606–1610.

(15) Zhang, P.; Zhang, L.; Wang, C.; Xue, S.; Lin, S. Y.; Tang, J. Equatorially Coordinated Lanthanide Single Ion Magnets. *J. Am. Chem. Soc.* **2014**, *136*, 4484–4487.

(16) Sun, W. B.; Yan, P. F.; Jiang, S. D.; Wang, B. W.; Zhang, Y. Q.; Li, H. F.; Chen, P.; Wang, Z. M.; Gao, S. High Symmetry or Low Symmetry, That Is the Question - High Performance Dy(III) Single-Ion Magnets by Electrostatic Potential Design. *Chem. Sci.* **2016**, 7, 684–691.

(17) Wu, J. F.; Jung, J. L.; Zhang, P.; Zhang, H. X.; Tang, J. K.; Le Guennic, B. *Cis-Trans* Isomerism Modulates the Magnetic Relaxation of Dysprosium Single-Molecule Magnets. *Chem. Sci.* **2016**, *7*, 3632–3639.

(18) Chen, Y. C.; Liu, J. L.; Ungur, L.; Liu, J.; Li, Q. W.; Wang, L. F.; Ni, Z. P.; Chibotaru, L. F.; Chen, X. M.; Tong, M. L. Symmetry-Supported Magnetic Blocking at 20 K in Pentagonal

Bipyramidal Dy (III) Single-Ion Magnets. *J. Am. Chem. Soc.* **2016**, *138*, 2829–2837.

(19) Liu, J.; Chen, Y. C.; Liu, J. L.; Vieru, V.; Ungur, L.; Jia, J. H.; Chibotaru, L. F.; Lan, Y.; Wernsdorfer, W.; Gao, S.; Chen, X. M.; Tong, M. L. A Stable Pentagonal Bipyramidal Dy (III) Single-Ion Magnet with a Record Magnetization Reversal Barrier Over 1000 K. *J. Am. Chem. Soc.* **2016**, *138*, 5441–5450.

(20) Ding, Y. S.; Chilton, N. F.; Winpenny, R. E. P.; Zheng, Y. Z. On Approaching the Limit of Molecular Magnetic Anisotropy: A Near-Perfect Pentagonal Bipyramidal Dysprosium(III) Single-Molecule Magnet. *Angew. Chem. Int. Ed.* **2016,** *55*, 16071–16074.

(21) Hewitt, I. J.; Tang, J. K.; Madhu, N. T.; Anson, C. E.; Lan, Y. H., Luzon, J.; Etienne, M.; Sessoli, R.; Powell, A. K. Coupling Dy_3 Triangles Enhances Their Slow Magnetic Relaxation. *Angew. Chem. Int. Ed.* **2010**, 49, 6352-6356.

(22) Guo, Y. N.; Xu, G. F.; Gamez, P.; Zhao, L.; Lin, S. Y.; Deng, R. P.; Tang, J. K.; Zhang, H.-J. Two-Step Relaxation in a Linear Tetranuclear Dysprosium(III) Aggregate Showing Single-Molecule Magnet Behavior. *J. Am. Chem. Soc.* **2010***, 132,* 8538–8539.

(23) Blagg, R. J.; Ungur, L.; Tuna, F.; Speak, J.; Comar, P.; Collison, D.; Wernsdorfer, W.; McInnes, E. J. L.; Chibotaru, L. F.; Winpenny, R. E. P. Magnetic Relaxation Pathways in Lanthanide Single-Molecule Magnets. *Nat. Chem.* **2013**, *5*, 673–678.

(24) Pineda, E. M.; Chilton, N. F.; Marx, R.; Dörfel, M.; Sells, D. O.; Neugebauer, P.; Jiang, S. D.; Collison, D.; Slageren, J. V.; McInnes, E. J. L.; Winpenny, R. E.P. Direct Measurement of Dysprosium(III)···Dysprosium(III) Interactions in a Single-Molecule Magnet. *Nat. Commun.* **2014**, *5*, 5243.

(25) Xiong, J.; Ding, H. Y.; Meng, Y. S.; Gao, C.; Zhang, X. J.; Meng, Z. S.; Zhang, Y. Q.; Shi, W.; Wang, B. W.; Gao, S. Hydroxide-Bridged Five-Coordinate Dy^{III} Single-Molecule

Magnet Exhibiting the Record Thermal Relaxation Barrier of Magnetization among Lanthanide-Only Dimers. *Chem. Sci.* **2017**, *8*, 1288–1294.

(26) Giansiracusa, M. J.; Moreno-Pineda, E.; Hussain, R.; Marx, R.; Prada, M. M.; Neugebauer, P.; Al-Badran, S.; Collison, D.; Tuna, F.; Slageren, J.; Carretta, S.; Guidi, T.; McInnes, E. J. L.; Winpenny, R. E. P.; Chilton, N. F. Measurement of Magnetic Exchange in Asymmetric Lanthanide Dimetallics: Toward a Transferable Theoretical Framework. *J. Am. Chem. Soc.* **2018**, *140*, 2504–2513.

(27) Guo, Y. N.; Xu, G. F.; Wernsdorfer, W.; Ungur, L.; Guo, Y.; Tang, J. K.; Zhang, H. J.; Chibotaru, L. F.; Powell, A. K. Strong Axiality and Ising Exchange Interaction Suppress Zero-Field Tunneling of Magnetization of an Asymmetric Dy_2 Single-Molecule Magnet. *J. Am. Chem. Soc.* **2011**, *133*, 11948–11951.

(28) Rinehart, J. D.; Fang, M.; Evans, W. J.; Long, J. R. Strong Exchange and Magnetic Blocking in N_2^{3-}-Radical-Bridged Lanthanide Complexes. *Nat. Chem.* **2011**, *3*, 538–542.

(29) Zhang, L.; Zhang, Y. Q.; Zhang, P.; Zhao, L.; Guo, M.; Tang, J. K. Single-Molecule Magnet Behavior Enhanced by Synergic Effect of Single-Ion Anisotropy and Magnetic Interactions. *Inorg. Chem.* **2017**, *56*, 7882–7889.

(30) Song, Y. M.; Luo, F.; Luo, M. B.; Liao, Z. W.; Sun, G. M.; Tian, X. Z.; Zhu, Y.; Yuan, Z. J.; Liu, S. J.; Xu, W. Y.; Feng, X. F. The Application of Single-Crystal-to-Single-Crystal Transformation Towards Adjustable SMM Properties. *Chem. Commun.* **2012**, *48*, 1006–1008.

(31) Wang, Y.-L.; Han, C.-B.; Zhang, Y.-Q.; Liu, Q.-Y.; Liu, C.-M.; Yin, S.-G. Fine-Tuning Ligand to Modulate the Magnetic Anisotropy in a Carboxylate-Bridged Dy_2 Single-Molecule Magnet System. *Inorg. Chem.* **2016**, *55*, 5578–5584.

(32) Mondal, K. C.; Kostakis, G. E.; Lan, Y. H.; Powell, A. K. Magnetic Properties of Five

Planar Defect Dicubanes of $[Ln^{III}_4(\mu_3\text{-}OH)_2(L)_4(HL)_2]\cdot 2THF$ (Ln = Gd, Tb, Dy, Ho and Er). *Polyhedron* **2013**, *66*, 268–273.

(33) Zhang, H. F.; Zhang, J.; Li, Y. H.; Qin, Y. R.; Chen, Y. M.; Liu, W.; Gao, D. D.; Li, W. A Series of Tetranuclear $[Ln_4]$ Clusters with Defect-Dicubane Cores Including a Dy_4 Single-Molecule Magnet. *J. Coord. Chem.* **2015**, *68*, 2798–2809.

(34) Liu, T. Q.; Yan, P. F.; Luan, F.; Li, Y. X.; Sun, J. W.; Chen, C.; Yang, F.; Chen, H.; Zou, X. Y.; Li, G. M. Near-IR Luminescence and Field-Induced Single Molecule Magnet of Four Salen-Type Ytterbium Complexes. *Inorg. Chem.* **2015**, 54, 221–228.

(35) Zhang, K.; Kurmoo, M.; Wei, L. Q.; Zeng, M. H. Iterative Mass Spectrometry and X-Ray Crystallography to Study Ion-Trapping and Rearrangements by a Flexible Cluster. *Sci. Rep.* **2013**, *3*, 3516.

(36) Zhang, K.; Yuan, C.; Guo, F. S.; Zhang, Y. Q.; Wang, Y. Y. Fine-Tuning Terminal Solvent Ligands to Rationally Enhance the Energy Barrier in Dinuclear Dysprosium Single-Molecule Magnets. *Dalton Trans.* **2017**, *46*, 186–192.

(37) Zhang, K.; Liu, D.; Vieru, V.; Hou, L.; Cui, B.; Guo, F. S.; Chibotaru, L. F.; Wang, Y. Y. Transitions of Two Magnetic Interaction States in Dinuclear Dy(III) Complexes *via* Subtle Structural Variations. *Dalton Trans.* **2017**, *46*, 638–642.

(38) Zhang, K.; Guo, F. S.; Wang, Y. Y. Two $\{Dy_2\}$ Single-Molecule Magnets Formed *via* an *In Situ* Reaction by Capturing CO_2 from Atmosphere under Ambient Conditions. *Dalton Trans.* **2017**, *46*, 1753–1756.

(39) Zheng, Y Z.; Lan, Y.; Anson, C. E.; Powell, A.K. Anion-Perturbed Magnetic Slow Relaxation in Planar $\{Dy_4\}$ Clusters. *Inorg. Chem.* **2008**, *47*, 10813–10815.

(40) Lin, P. H.; Burchell, T. J.; Ungur, L.; Chibotaru, L. F.; Wernsdorfer, W.; Murugesu, M. A

Polynuclear Lanthanide Single-Molecule Magnet with a Record Anisotropic Barrier. *Angew. Chem., Int. Ed.* **2009**, *48*, 9489–9492.

(41) Abbas, G.; Lan, Y.; Kostakis, G. E.; Wernsdorfer, W.; Anson, C. E.; Powell, A. K. Series of Isostructural Planar Lanthanide Complexes $[Ln^{III}_4(M_3\text{-}OH)_2(Mdeah)_2(Piv)_8]$ with Single Molecule Magnet Behavior for the Dy_4 Analogue. *Inorg. Chem.* **2010**, *49*, 8067–8072.

(42) Yan, P. F.; Lin, P. H.; Habib, F.; Aharen, T.; Murugesu, M.; Deng, Z. P.; Li, G. M.; Sun, W. B. Planar Tetranuclear Dy (III) Single-Molecule Magnet and Its Sm (III), Gd (III), and Tb (III) Analogues Encapsulated by Salen-Type and β-Diketonate Ligands. *Inorg. Chem.* **2011**, *50*, 7059-7065.

(43) Chandrasekhar, V.; Hossain, S.; Das, S.; Biswas, S.; Sutter, J. P. Rhombus-Shaped Tetranuclear $[Ln_4]$ Complexes [Ln= Dy (III) and Ho (III)]: Synthesis, Structure, and SMM Behavior. *Inorg. Chem.* **2013**, *52*, 6346–6353.

(44) Luan, F.; Liu, T. Q.; Yan, P. F.; Zou, X. Y.; Li, Y. X.; Li. G. M. Single-Molecule Magnet of a Tetranuclear Dysprosium Complex Disturbed by a Salen-Type Ligand and Chloride Counterions. *Inorg. Chem.* **2015**, *54*, 3485–3490.

(45) Luan, F.; Yan, P. F.; Zhu, J.; Liu, T. Q.; Zou, X. Y.; Li. G. M. A Salen-Type Dy_4 Single-Molecule Magnet with an Enhanced Energy Barrier and Its Analogues. *Dalton Trans.* **2015**, *44*, 4046–4053.

(46) Xue, S.; Zhao, L.; Guo, Y. N.; Deng, R. P.; Guo, Y.; Tang, J. K. A Series of Tetranuclear Lanthanide Complexes Comprising Two Edge-Sharing Triangular Units with Field-Induced Slow Magnetic Relaxation for Dy_4 species. *Dalton Trans.* **2011**, *40*, 8347–8352.

(47) Llunell, M.; Casanova, D.; Cirera, J.; Alemany, P.; Alvarez, S. *Shape v. 2.1*, Universitat de Barcelona, Barcelona, **2013**.

(48) Miras, H. N.; Wilson, E. F.; Cronin, L. Unravelling the Complexities of Inorganic and Supramolecular Self-Assembly in Solution with Electrospray and Cryospray Mass Spectrometry. *Chem. Commun.* **2009**, *0*, 1297–1311.

(49) Jiang, W.; Schäfer, A.; Mohr, P. C.; Schalley, C. A. Monitoring Self-Sorting by Electrospray Ionization Mass Spectrometry: Formation Intermediates and Error-Correction during the Self-Assembly of Multiply Threaded Pseudorotaxanes. *J. Am. Chem. Soc.* **2010**, *132*, 2309–2320.

(50) Kahn, O. *Molecular Magnetism*, Wiley-VCH, New York, **1993**.

(51) Kahn, M. L.; Sutter, J. P.; Golhen, S.; Guionneau, P.; Ouahab, L.; Kahn, O.; Chasseau, D. Systematic Investigation of the Nature of the Coupling between a Ln(III) Ion (Ln = Ce(III) to Dy(III)) and Its Aminoxyl Radical Ligands. Structural and Magnetic Characteristics of a Series of {Ln(organic radical)$_2$} Compounds and the Related {Ln(Nitrone)$_2$} Derivatives. *J. Am. Chem. Soc.*, **2000**, *122*, 3413–3421.

(52) Gao, H. L.; Zhou, X. P.; Bi, Y. X.; Shen, H. Y.; Wang, W. M.; Wang, N. N.; Chang, Y. X.; Zhang, R. X.; Cui, J. Z. A Dy_4 Single-Molecule Magnet and Its Gd(III), Tb(III), Ho(III), And Er(III) Analogues Encapsulated by an 8-Hydroxyquinoline Schiff Base Derivative and β-Diketonate Coligand. *Dalton Trans.* **2017**, *46*, 4669–4677.

(53) Aquilante, F.; Autschbach, J.; Carlson, R. K.; Chibotaru, L. F.; Delcey, M. G.; De Vico, L.; Galván, I. F.; Ferré, N.; Frutos, L. M.; Gagliardi, L.; Garavelli, M.; Giussani, A.; Hoyer, C. E.; Manni, G. L.; Lischka, H.; Ma, D. X.; Malmqvist, P.; Müller, T.; Nenov, A.; Olivucci, M.; Pedersen, T. B.; Peng, D. L.; Plasser, F.; Pritchard, B.; Reiher, M.; Rivalta, I.; Schapiro, I.; Segarra-Martí, J.; Stenrup, M.; Truhlar, D. G.; Ungur, L.; Valentini, A.; Vancoillie, S.; Veryazov, V.; Vysotskiy, V. P.; Weingart, O.; Zapata, F.; Lindh, R. Molcas 8: New Capabilities

for Multiconfigurational Quantum Chemical Calculations Across the Periodic Table. *J. Comput. Chem.* **2016**, *37*, 506–541.

(54) Zhang, X.; Vieru, V.; Feng, X.; Liu, J. L.; Zhang, Z.; Na, B.; Shi, W.; Wang, B. W.; Powell, A. K.; Chibotaru, L. F.; Gao, S.; Cheng, P.; Long, J. R. Influence of Guest Exchange on the Magnetization Dynamics of Dilanthanide Single-Molecule-Magnet Nodes within a Metal-Organic Framework. *Angew. Chem., Int. Ed.* **2015**, *54*, 9861–9865.

(55) Gatteschi, D.; Sessoli, R.; Vallain, J. *Molecular Nanomagnets*, Oxford University Press, New York, **2006**.

(56) Zhang, L.; Jung, J.; Zhang, P.; Guo, M.; Zhao, L.; Tang, J. K.; Le Guennic, B. Site-Resolved Two-Step Relaxation Process in an Asymmetric Dy_2 Single-Molecule Magnet. *Chem.-Eur. J.* **2016**, *22*, 1392–1398.

(57) Zhao, L. L.; Guo, Y. N.; Yu, G. M.; Guo, Y.; Tang, J. K.; Li, Y. H. A Dodecanuclear Heterometallic Dysprosium–Cobalt Wheel Exhibiting Single-Molecule Magnet Behaviour. *Chem. Commun.* **2011**, *47*, 8659–8661.

Table of Contents Graphic

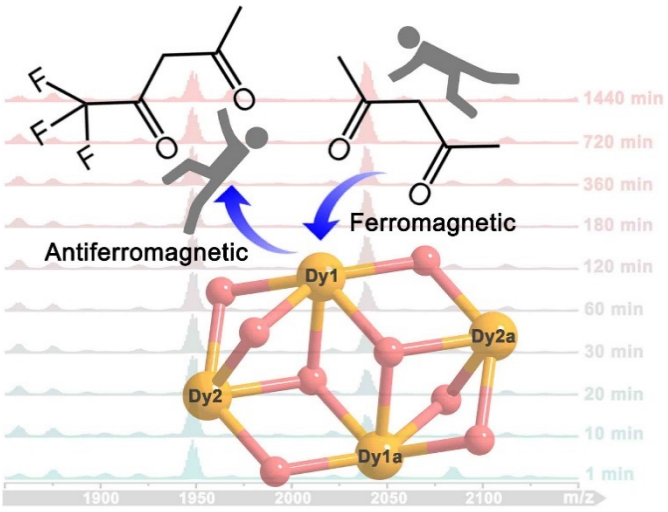

Structural variations within three tetranuclear Dy(III) SMMs have been demonstrated to impart major changes in the magnetic interactions. *Ab initio* calculations revealed that changes in the coordination environment around Dy(III) can significantly affect magnetic interactions.